Supplementary Information for

Three-dimensional climatology, trends and meteorological drivers of global and regional tropospheric type-dependent aerosols: Insights from 13 years (2007–2019) of CALIOP observations

5 Ke Gui[1], Huizheng Che[1*], Yu Zheng[1], Hujia Zhao[2], Wenrui Yao[1], Lei Li[1], Lei Zhang[1], Hong Wang[1], Yaqiang Wang[1], Xiaoye Zhang[1]

[1]State Key Laboratory of Severe Weather & Key Laboratory of Atmospheric
Chemistry of CMA, Chinese Academy of Meteorological Sciences, Beijing, 100081, China
[2]Institute of Atmospheric Environment, China Meteorological Administration, Shenyang, 110166, China

Correspondence to: Huizheng Che (chehz@cma.gov.cn)

Table S1. Classification of the 12 regions of interest (ROIs) in this study.

Region	Abbreviation	Latitude and longitude ranges
Eastern United States	EUS	73°W–94°W, 29°N–45°N
Western Europe	WEU	10°W–18°E, 37°N–59°N
Southern Asia	SA	72°E–90°E, 10°N–30°N
Northern China	NC	108°E–120°E, 30°N–40°N
Southern China	SC	108°E–120°E, 20°N–30°N
Northeastern Asia	NEA	125°E–145°E, 30°N–41°N
Sahara Desert	SD	17°W–20°E, 3°N–25°N
Middle East	ME	38°E–56°E,14°N–33°N
Northwestern China	NWC	73°E–94°E, 35°N–47°N
Amazon Zone	AMZ	46°W–60°W, 1°S–22°S
Central Southern Africa	CSA	12°E–33°E, 2°S–18°S
Southeastern Asia	SEA	96°E–127°E, 8°S–18°N
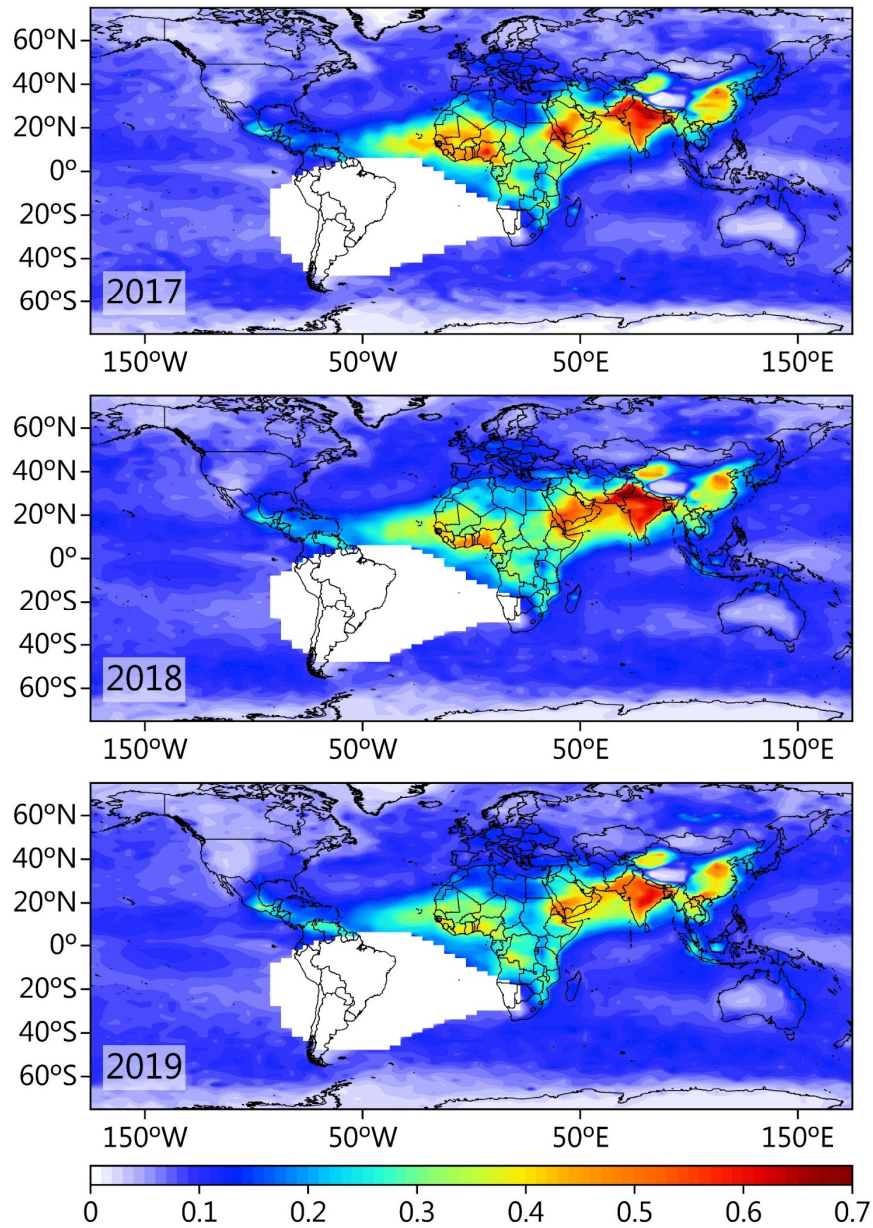
Figure S1. Areas within and near the South Atlantic anomaly region that have been excluded from this study due to an elevated frequency of low energy laser shots encountered by CALIOP since September 2016. The shading shows the annual distribution of TAOD for each year from 2017–2019, with the white areas corresponding to the South Atlantic anomaly areas encountered by CALIOP each year.
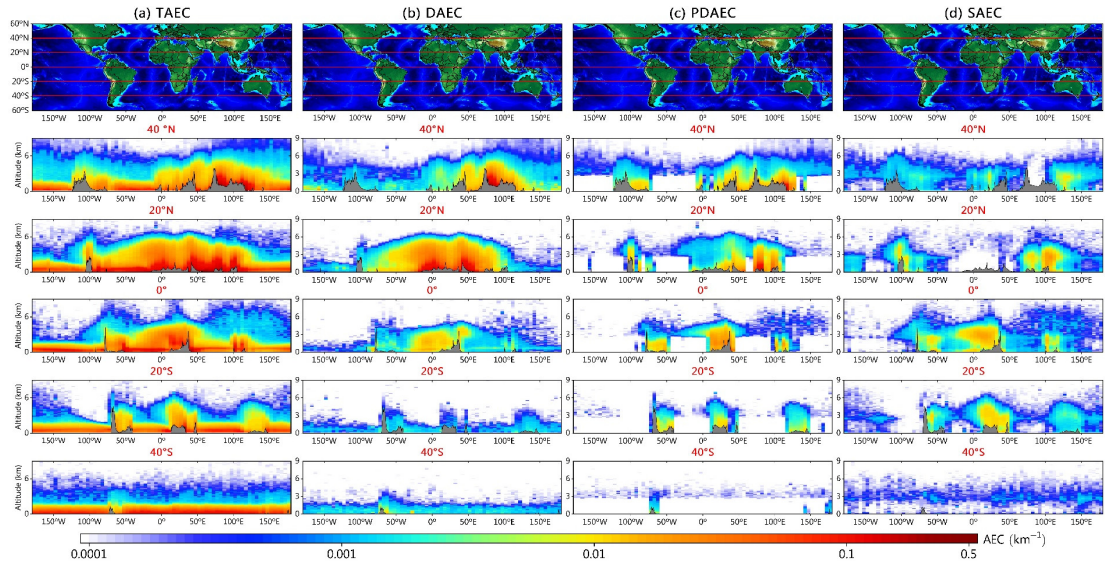
40 **Figure S2.** Zonal vertical profiles of multi-year (2007–2019) average aerosol extinction coefficients (AEC) due to type-dependent aerosols: (a) total aerosols, (b) dust, (c) polluted dust (PD), and (d) smoke. From top to bottom are 40°N, 20°N, 0°, 20°S, and 40°S, respectively.
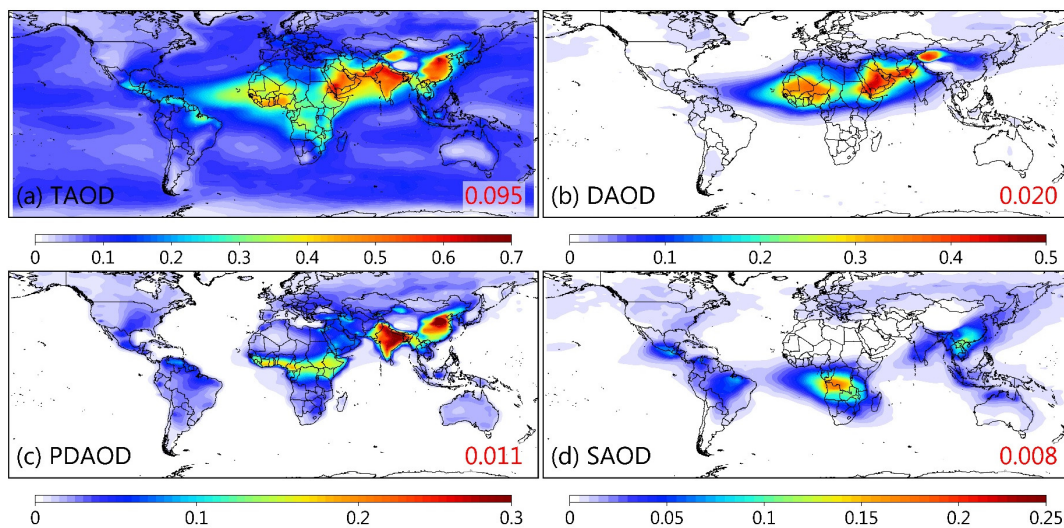
Figure S3. Spatial distributions of multi-year average AODs for (a) total aerosols, (b) dust, (c) PD, and (d) smoke. The number in the lower-right of each panel represents the global average.
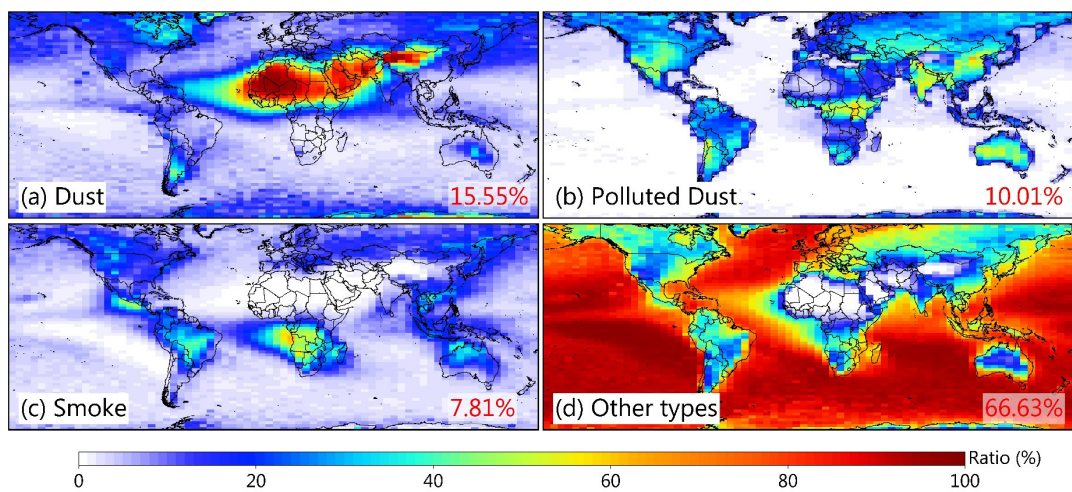
Figure S4. Spatial distributions of the multi-year average proportion of type-dependent AODs, including (a) dust, (b) PD, (c) smoke, and (d) other types, to total AOD. The number in the lower-right of each panel represents the global average.

55
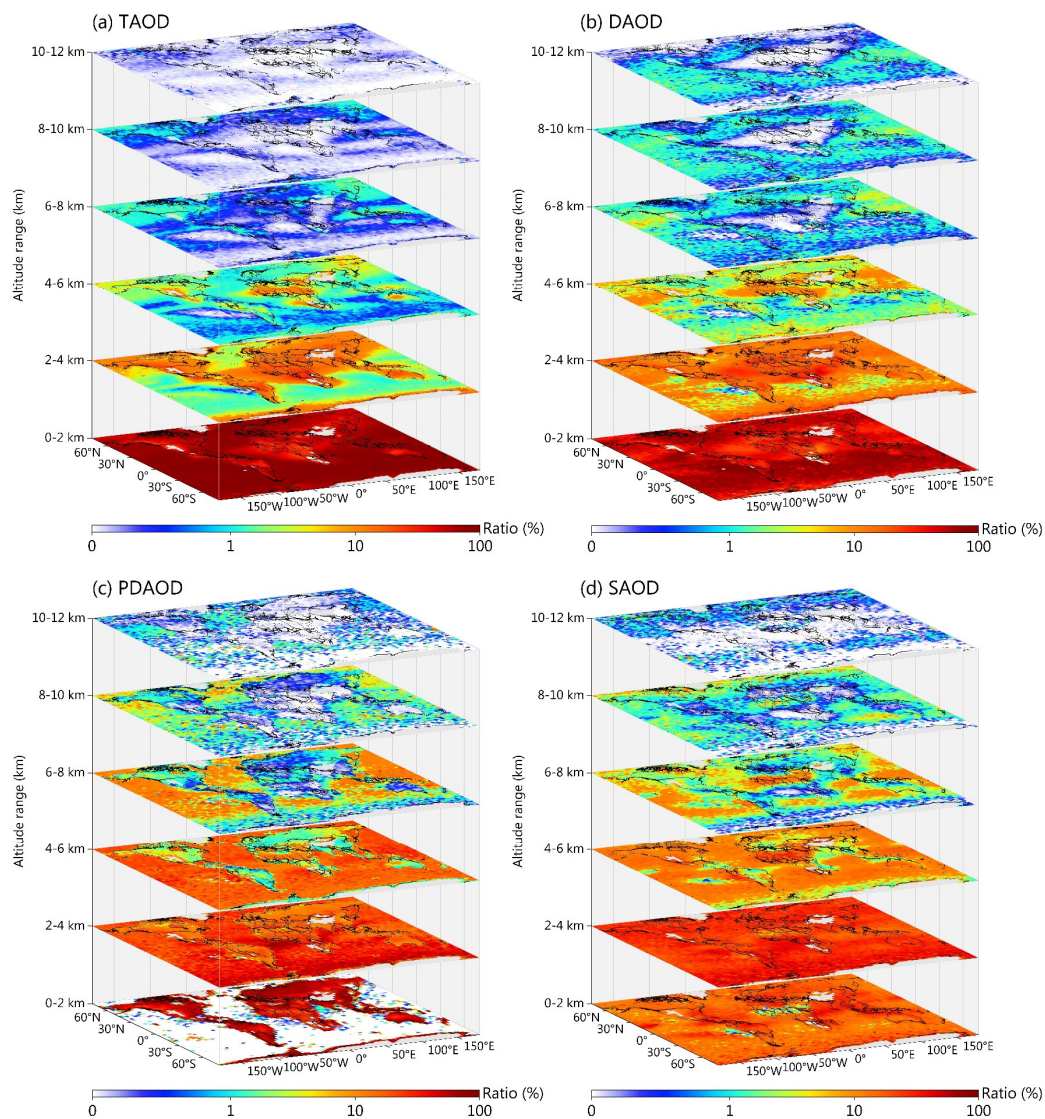
Figure S5. Spatial distributions of multi-year average proportions of type-dependent layer-specific (i.e., integrated at 2-km intervals from the surface to 12 km) AODs, including (a) total aerosols, (b) dust, (c) PD, and (d) smoke, to total type-dependent AODs.

60
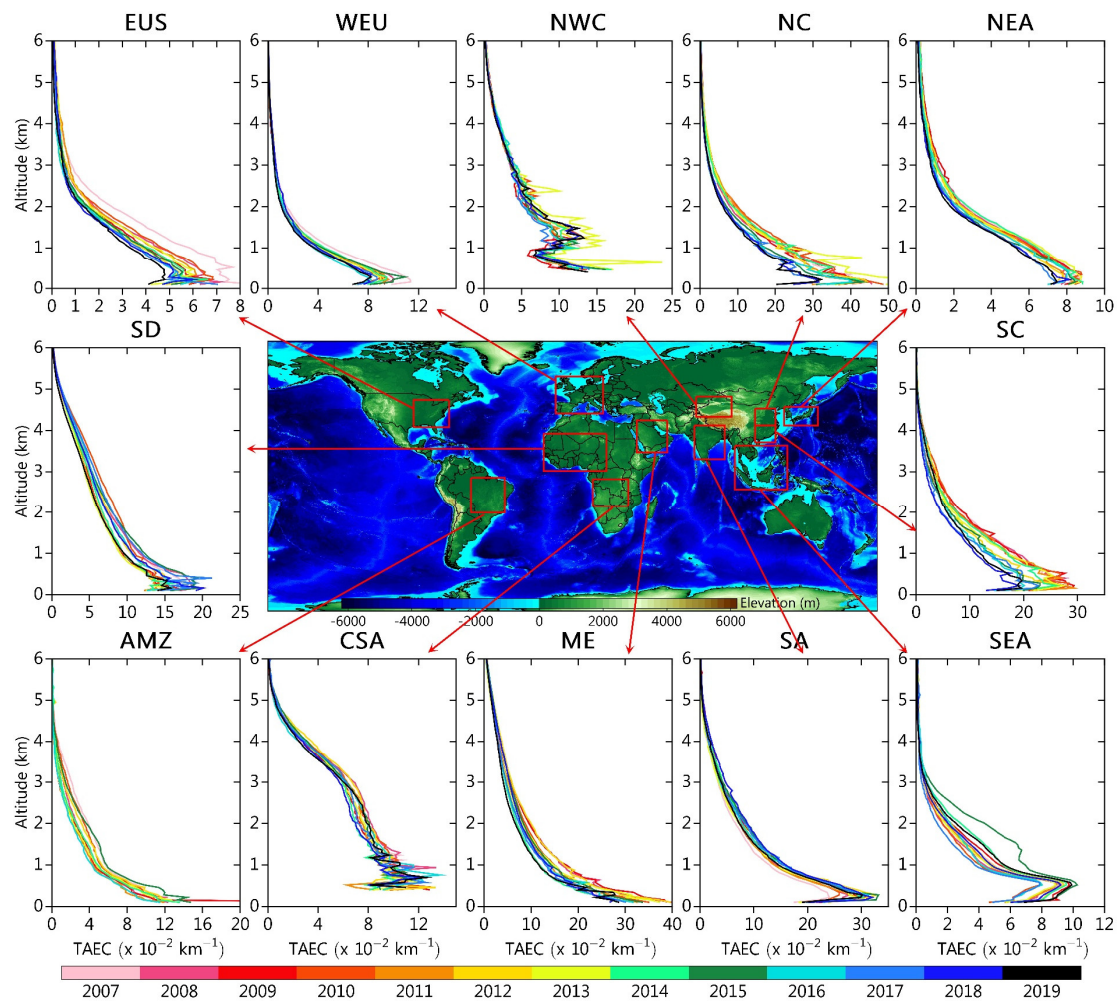
Figure S6. Interannual variations in regional-average vertical profiles of the total AEC over the 12 ROIs.
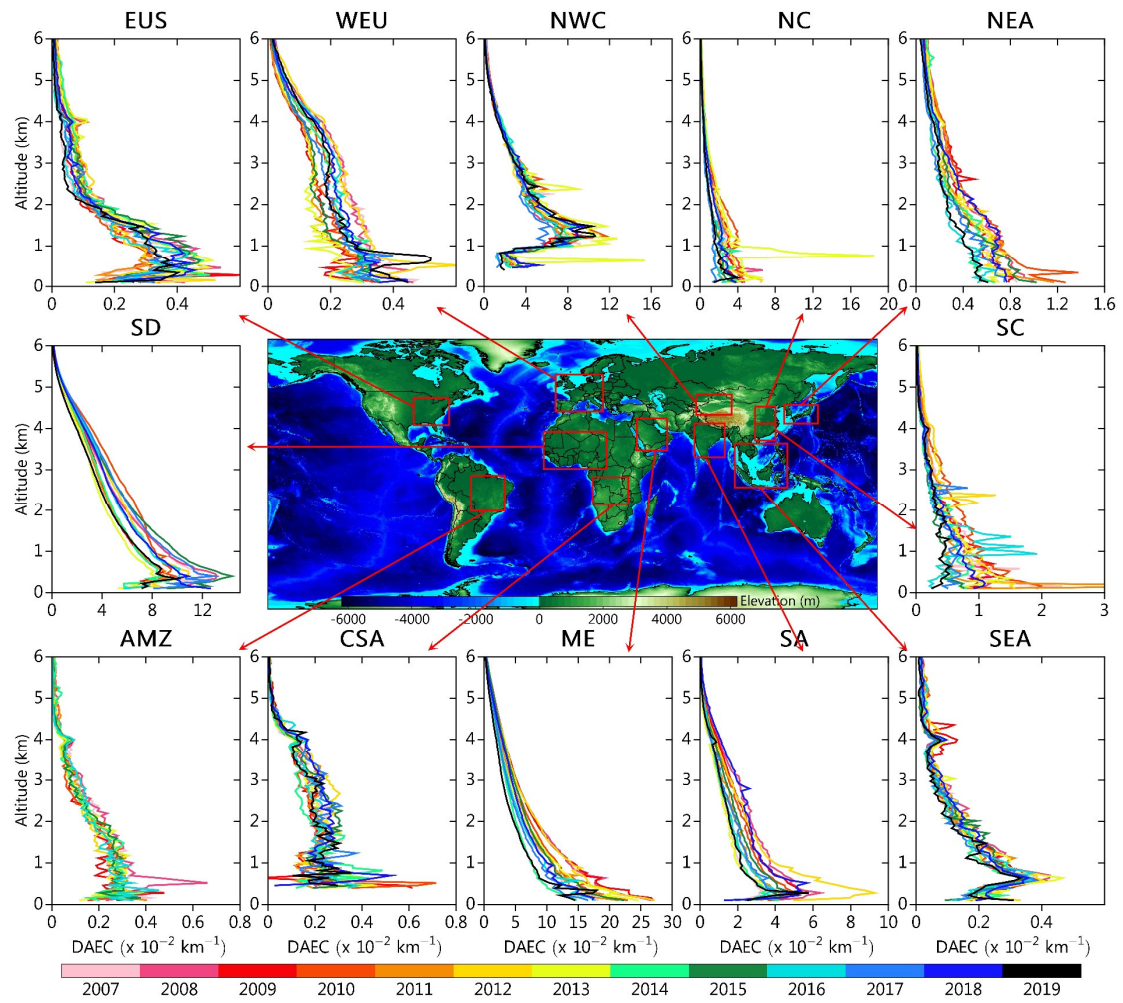
Figure S7. As in Figure S6 but for AEC due to dust.
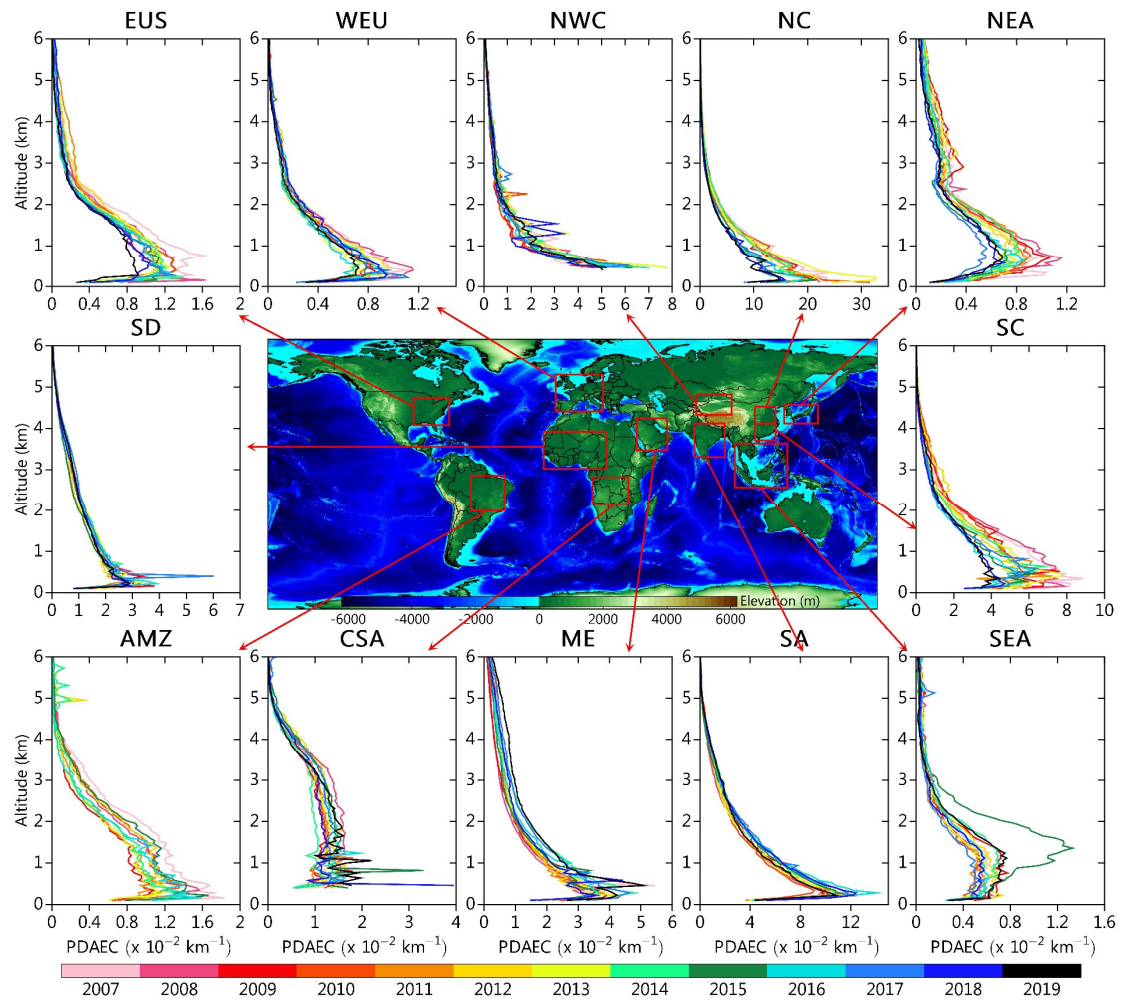
Figure S8. As in Figure S6 but for AEC due to PD.

70
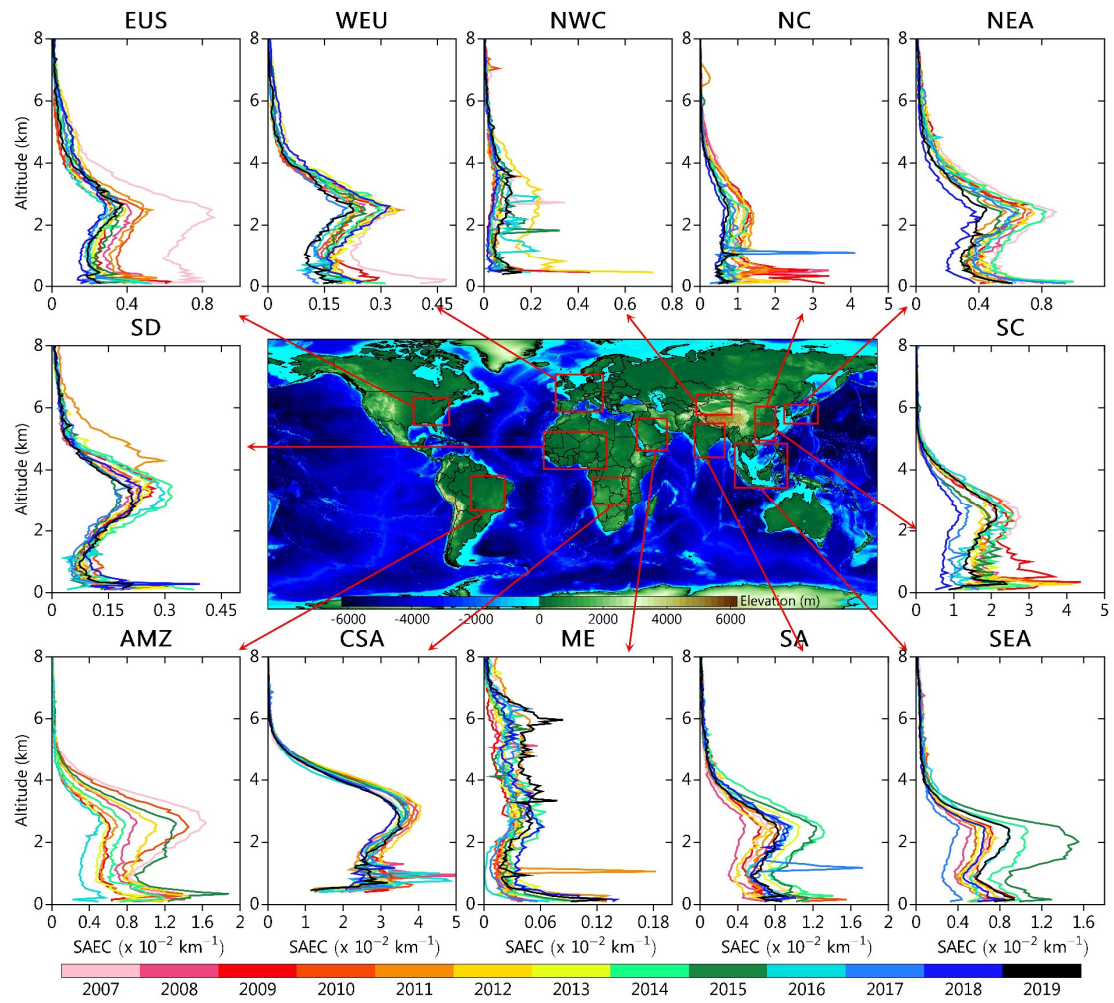
Figure S9. As in Figure S6 but for AEC due to smoke.
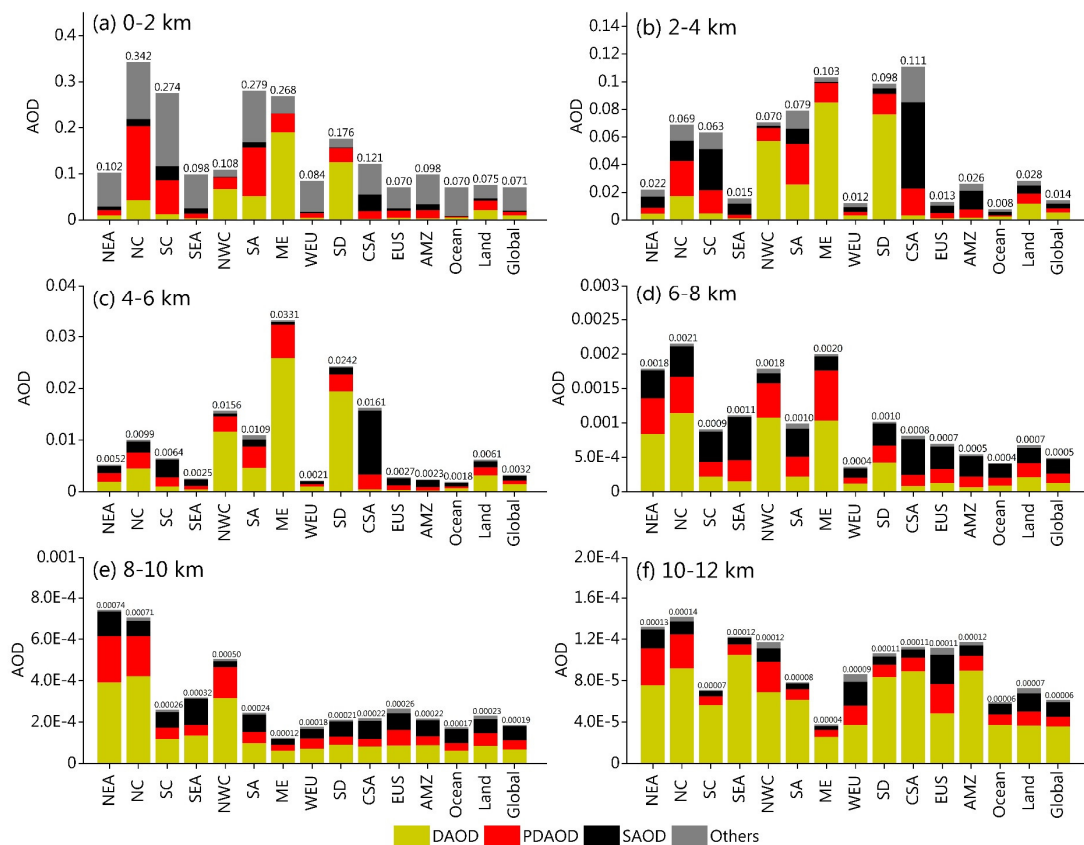
75 **Figure S10. Multi-year regional-average layer-specific type-dependent AODs integrated at (a) 0–2 km, (b) 2–4 km, (c) 4–6 km, (d) 6–8 km, (e) 8–10 km, and (f) 10–12 km.**
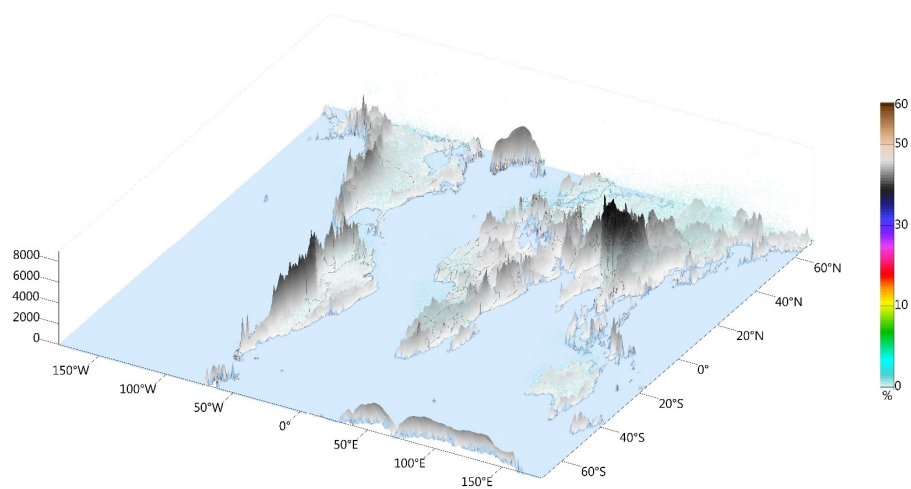
80

Figure S11. 3D particle map of the annual FoO for the clean continental (CC) averaged over 13 years (2007–2019).
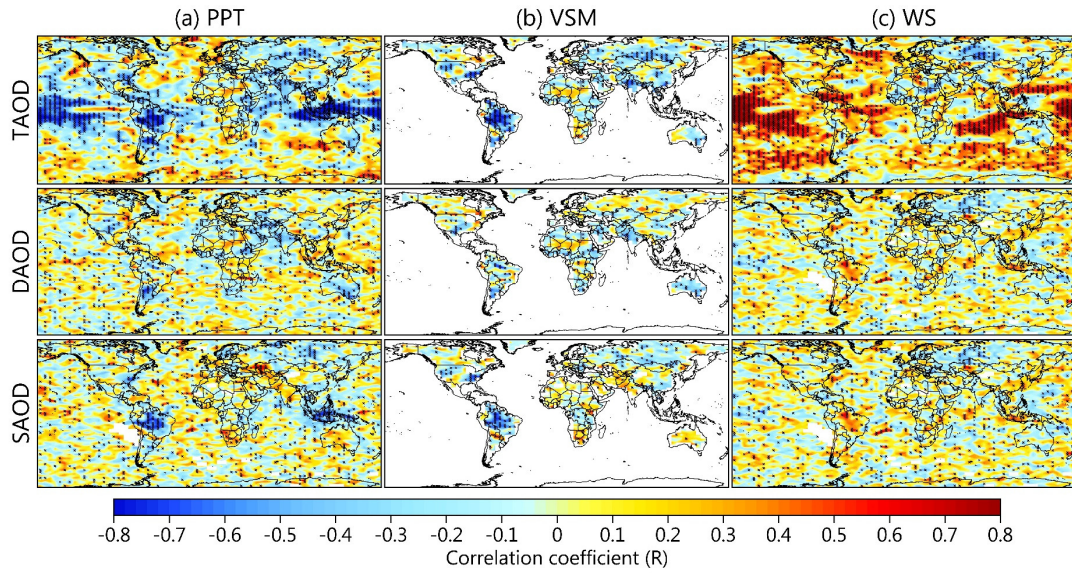
85 **Figure S12. Spatial distributions of the correlation coefficients (*R*) for TAOD, DAOD, and SAOD in the planetary boundary layer versus (a) precipitation (PPT), (b) volumetric soil moisture (VSM), and (c) wind speed at 10 m (WS) for 2007–2019. Note that the grids with *R* at a 90% significance level from the two-tailed Student's t-test are marked by black "×" symbols.**
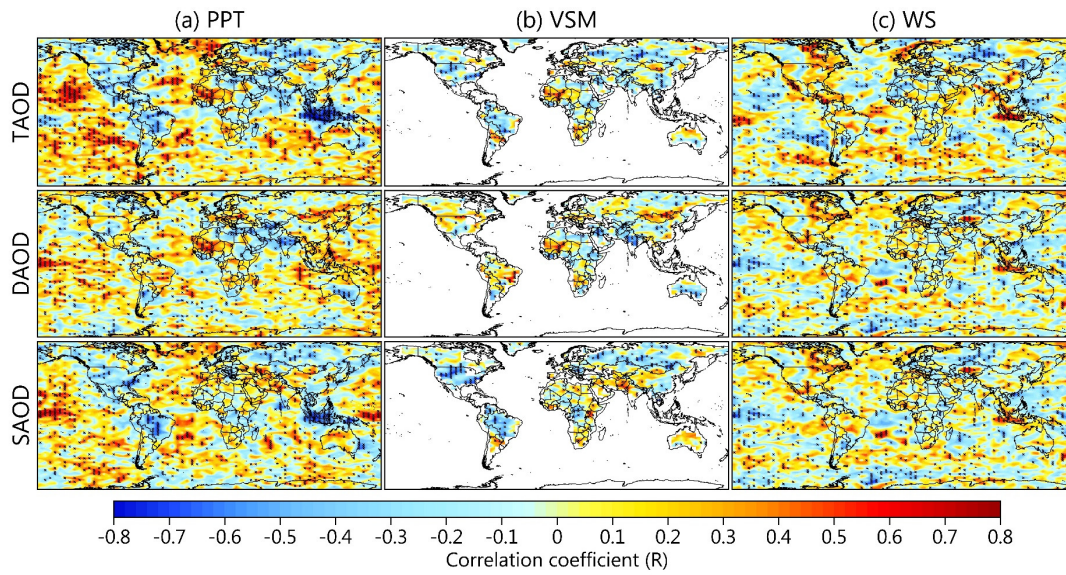
90   **Figure S13. Spatial distributions of the correlation coefficients (*R*) for TAOD, DAOD, and SAOD in the free troposphere versus (a) PPT, (b) VSM, and (c) WS for 2007–2019. Note that the grids with *R* at a 90% significance level from the two-tailed Student's t-test are marked by black "×" symbols.**